Acigöl rhyolite field, Central Anatolia (part 1): high-resolution dating of eruption episodes and zircon growth rates

Axel K. Schmitt, Martin Danišík, Noreen J. Evans, Wolfgang Siebel, Elena Kiemele, Faruk Aydin & Janet C. Harvey

Contributions to Mineralogy and Petrology

ISSN 0010-7999
Volume 162
Number 6

Contrib Mineral Petrol (2011)
162:1215-1231
DOI 10.1007/s00410-011-0648-x

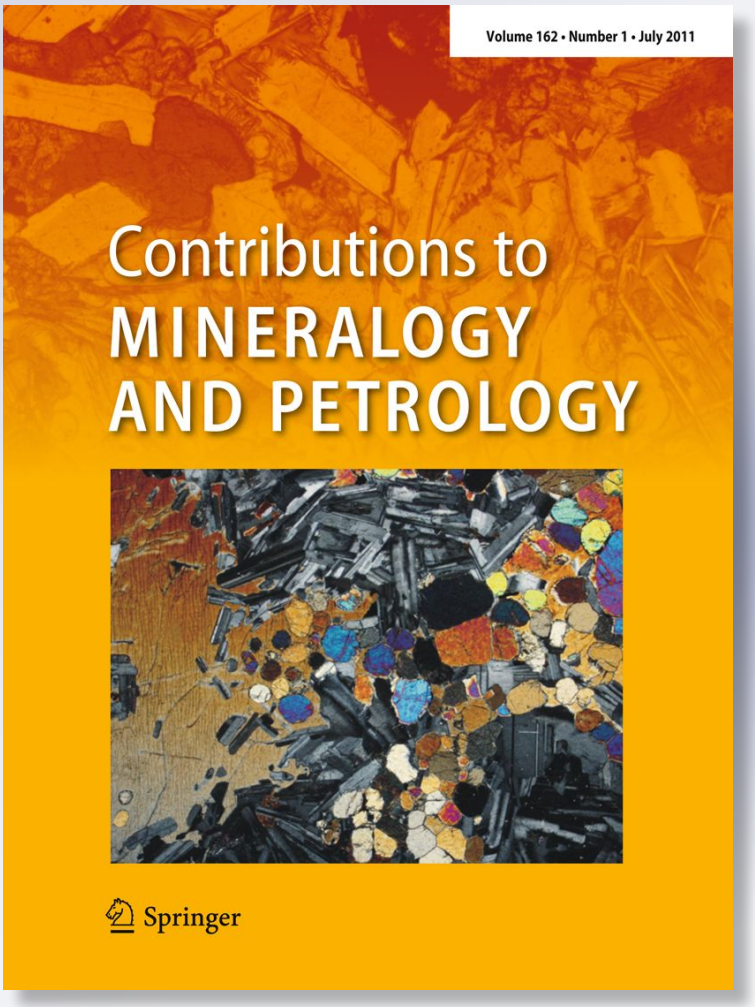

Springer

Contrib Mineral Petrol (2011) 162:1215–1231
DOI 10.1007/s00410-011-0648-x

ORIGINAL PAPER

Acigöl rhyolite field, Central Anatolia (part 1): high-resolution dating of eruption episodes and zircon growth rates

Axel K. Schmitt · Martin Danišík · Noreen J. Evans · Wolfgang Siebel · Elena Kiemele · Faruk Aydin · Janet C. Harvey

Received: 22 January 2011 / Accepted: 3 May 2011 / Published online: 24 May 2011

Abstract Protracted pre-eruptive zircon residence is frequently detected in continental rhyolites and can conflict with thermal models, indicating briefer magma cooling durations if scaled to erupted volumes. Here, we present combined U-Th and (U-Th)/He zircon ages from the Acigöl rhyolite field (Central Anatolia, Turkey), which is part of a Quaternary bimodal volcanic complex. Unlike other geochronometers, this approach dates crystallization and eruption on the same crystals, allowing for internal consistency testing. Despite the overall longevity of Acigöl rhyolite volcanism and systematic trends of progressive depletion in compatible trace elements and decreasing zircon saturation temperatures, we find that zircon crystallized in two brief pulses corresponding to eruptions in the eastern and western part of the field during Middle and Late Pleistocene times, respectively. For Late Pleistocene zircon, resolvable differences exist between interior (average: 30.7 ± 0.9 ka; 1σ error) and rim (21.9 ± 1.3 ka) crystallization ages. These translate into radial crystal growth rates of $\sim 10^{-13}$ to 10^{-14} cm/s, broadly consistent with those constrained by diffusion experiments. Rim crystallization and (U-Th)/He eruption ages (24.2 ± 0.4 ka) overlap within uncertainty. Evidence for brief zircon residence at Acigöl contrasts with many other rhyolite fields, suggesting that protracted zircon crystallization in, or recycling from, long-lived crystal mushes is not ubiquitous in continental silicic magma systems. Instead, the span of pre-eruptive zircon ages is consistent with autochthonous crystallization in individual small-volume magma batches that originated from basaltic precursors.

Communicated by J. Hoefs.

Electronic supplementary material The online version of this article (doi:10.1007/s00410-011-0648-x) contains supplementary material, which is available to authorized users.

A. K. Schmitt (✉)
Department of Earth and Space Sciences,
University of California, Los Angeles, 595 Charles Young Drive East, Los Angeles, CA 90095-1567, USA
e-mail: axel@argon.ess.ucla.edu

M. Danišík · N. J. Evans
John de Laeter Centre for Isotope Research, Applied Geology,
Curtin University, GPO Box U1987, Perth, WA 6845, Australia

Present Address:
M. Danišík
Department of Earth and Ocean Sciences, Faculty of Science & Engineering, The University of Waikato, Private Bag 3105, Hamilton 3240, New Zealand

N. J. Evans
CSIRO Earth Science and Resource Engineering,
PO Box 1130, Bentley, WA 6102, Australia

W. Siebel · E. Kiemele
Institute of Geosciences, Universität Tübingen,
Wilhelmstr. 56, 72074 Tübingen, Germany

F. Aydin
Department of Geological Engineering, Karadeniz Technical University, 61010 Campus Trabzon, Turkey

J. C. Harvey
Geological and Planetary Sciences, California Institute of Technology, MC 170-25, 1200 E California Blvd,
Pasadena, CA 91125, USA

Keywords Zircon · (U-Th)/He · Uranium series · Calderas · Rhyolite domes

Introduction

Continental rhyolite fields are the surface expression of intra-crustal hot zones capable of producing protracted (over hundred of thousands or million years) and cumulatively voluminous outpourings of differentiated magma, as well as batholith-sized intrusive bodies. They are often temporally and spatially associated with basaltic eruptions forming bimodal complexes. Absence of basaltic vents in rhyolite-dominated regions has been interpreted as evidence for an underlying partially molten crustal density filter preventing mantle-derived magmas from reaching the surface (Bacon 1985; Druitt et al. 1995). Models emphasizing fractional crystallization of mafic magmas at shallow depth (~5 km) can explain first-order chemical characteristics of continental rhyolites (e.g., Fowler and Spera 2010), but crystal-chemical evidence from major and accessory phases (e.g., Reid et al. 2011) is frequently at odds with simple monotonic cooling scenarios and suggest episodic re-heating and mixing events. Moreover, the longevity of rhyolite fields and the explanation as to why some rhyolite systems oscillate between protracted small-volume monogenetic lava dome effusion and catastrophic caldera-forming eruptions remain poorly understood.

To better constrain the magmatic evolution of continental rhyolite fields and associated intra-crustal hot zones, we initiated a comprehensive investigation into the Acigöl complex in Cappadocia (Central Anatolia, Turkey; Fig. 1; see also Siebel et al. 2011). Unlike many other intra-continental rhyolite fields (e.g., Yellowstone, Long Valley), Acigöl lacks a giant caldera and therefore excellently preserves evidence of most of its eruptive history. Moreover, Acigöl is one of the youngest known rhyolite fields, similar to or even younger than Coso (California) which is also dominated by small-volume effusive eruptions (e.g., Bacon et al. 1981; Duffield et al. 1980; Simon et al. 2009). Because of its young age, dating of the eruptive stratigraphy and pre-eruptive crystallization can be achieved at high absolute temporal precision approaching millennial timescales, which is precluded in older rhyolite fields (e.g., Duffield and Dalrymple 1990). Combined U-Th and (U-Th)/He dating of individual zircon crystals provides a detailed chronostratigraphic record with the advantage over other Quaternary geochronometers (e.g., ^{14}C, $^{40}Ar/^{39}Ar$) of using the same crystals for dating crucial events in the evolution of the system (i.e., crystallization and eruption). This allows for an internal consistency check of the ages.

Our data permit testing of several hypotheses regarding rhyolite fields as an important end-member in the spectrum of continental magmatism: (1) dome clusters have multiple vents tapping a large underlying melt zone vs. individual feeding dikes that extend from a central magma body (e.g., Bacon 1985); (2) magmas are extracted from intra-crustal hot zones undergoing thermal cycling rather than thermally retrograde liquid-dominated reservoirs (e.g., Annen 2009; Fowler and Spera 2010); and (3) the presence of evolved melts in intra-crustal mush zones is protracted (e.g., Bachmann and Bergantz 2004; 2008) vs. rhyolitic magmas accumulating rapidly via re-melting of solidified rocks or rapid differentiation of basalts (Bacon and Lowenstern 2005; Bindeman et al. 2001; Lowenstern et al. 2000; Schmitt et al. 2003). In a companion paper (Siebel et al.

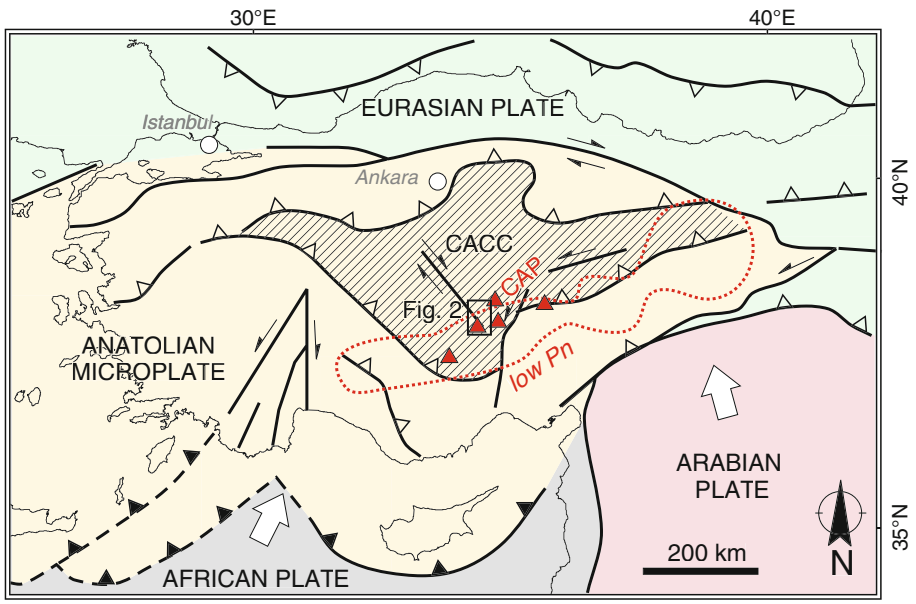

Fig. 1 Neotectonic overview map of Turkey with the location of the Cappadocian Volcanic Province (CVP) and its Holocene volcanoes (*red triangles*), as well as the distribution of basement rocks of the Central Anatolian Crystalline Complex (CACC; hatched). *Red dashed line* outlines low Pn velocity region in the upper mantle (Dilek and Sandvol 2009; Gans et al. 2009)

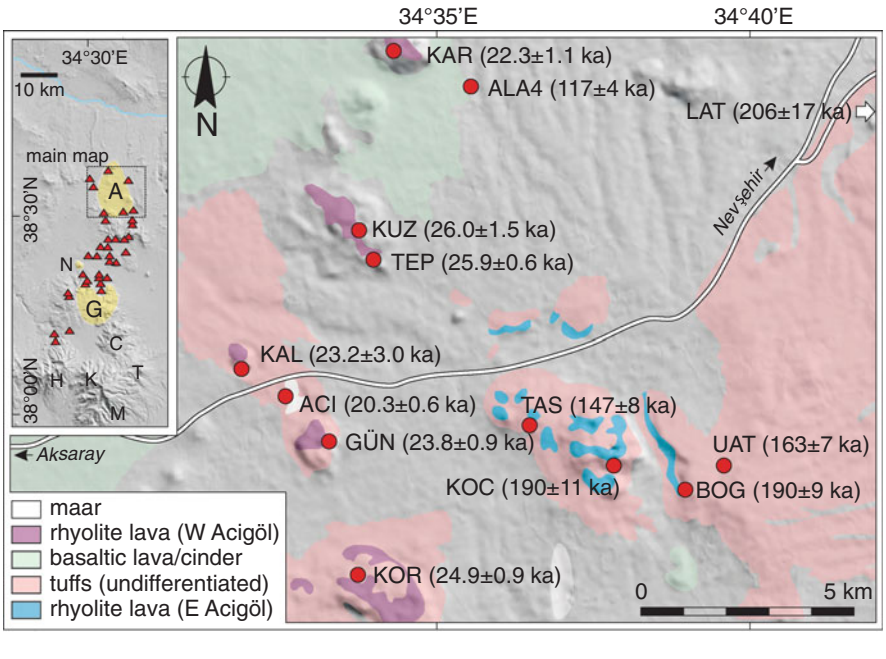

Fig. 2 Quaternary volcanic rocks (MTA 2005) overlay onto ASTER® global digital elevation model at 30-m lateral resolution. Sample locations and (U-Th)/He eruption ages are indicated. Inset: location of the Acigöl complex and the extent of the Lower and Upper Acigöl Tuffs (LAT and UAT, respectively) in relation to other Late Cenozoic volcanic units of the CVP (*yellow*: dominantly rhyolitic centers; *red triangles*: basaltic vents): *A* Acigöl, *N* Nenezi, *G* Göllüdağ, *C* Cinarli, *T* Tepeköy, *M* Melendiz, *K* Keçiboyduran, and *H* Hasan Dağı (after: Druitt et al. 1995; Gencalioglu-Kuscu and Geneli 2010)

2011), we present geochemical data (including radiogenic and oxygen isotope data) in support of evidence from zircon crystal-scale dating that precludes a seemingly straightforward crystal fractionation lineage between subsequently erupted rhyolites at Acigöl.

Geologic background

Cappadocian Volcanic Province

The Cappadocian Volcanic Province (CVP) is a ~300-km-long and ~40- to 100-km-wide NE-SW-oriented swath covering large areas within Central Anatolia (Fig. 1). Since about ~13.5 Ma, CVP volcanism has dominantly produced silicic ignimbrites, as well as intermediate lavas that erupted from stratovolcanic centers (Beekman 1966; Innocenti et al. 1975; Le Pennec et al. 1994; Pasquarè et al. 1988; Temel et al. 1998a, b). Miocene to Quaternary volcanic rocks cover crystalline basement comprising Paleozoic–Mesozoic metamorphic massifs, overthrusted by late Cretaceous Tethian ophiolites, and intruded by latest Cretaceous to early Cenozoic syn-collisional granitoids that are collectively termed the Central Anatolian Crystalline Complex (CACC), a major tectonic unit of Turkey (Dilek and Sandvol 2009; Gautier et al. 2008; Göncüoğlu 1986; Göncüoğlu and Toprak 1992). Neogene volcanism was synchronous with subsidence of fault-bounded basins that are filled with intercalated volcanogenic and terrigenous sediments (Dirik and Göncüoğlu 1996; Le Pennec et al. 1994; 2005; Mues-Schumacher et al. 2004; Temel et al. 1998b; Toprak 1998; Toprak and Göncüoğlu 1993; Viereck-Goette et al. 2010). The eruptive centers of Miocene–Pliocene ignimbrites inferred from field mapping and geophysical surveys are in close proximity to Quaternary rhyolite fields (Batum 1978; Dhont et al. 1998; Druitt et al. 1995; Froger et al. 1998; Le Pennec et al. 1994; Toprak 1998). The exact locations of older calderas, however, remain tenuous because they are largely covered by younger volcanic deposits.

The main focus of Quaternary rhyolite volcanism in the CVP is within an ~40-km-long and ~20-km-wide area comprising (from N to S) the Acigöl complex, the isolated Nenezi dome, and the Göllüdağ complex (Fig. 2). To the south of the Acigöl complex, ~100 Pleistocene-Holocene cinder cones, maars, and clusters of rhyolitic domes, coulees, and associated pyroclastic deposits (Aydar 1997; Batum 1978; Druitt et al. 1995; Ercan et al. 1991; Ercan et al. 1987; Mouralis et al. 2002) are superimposed onto remnants of Miocene to Pliocene stratovolcanoes (Aydin 2008; Ercan et al. 1992; Toprak 1998). Basaltic monogenetic centers are frequently aligned or elongated approximately N–S, suggesting parallel feeding dikes that opened perpendicular to the orientation of least principal stress (Batum 1978; Dhont et al. 1998; Druitt et al. 1995; Toprak 1998; Toprak and Göncüoğlu 1993). Vent alignment of the silicic domes within the rhyolite fields is seemingly irregular, and a systematic lack of basaltic vents within the field (a "basaltic shadow zone") has been interpreted to indicate the presence of low-density silicic intrusions or magma at depth acting as buoyancy traps for basaltic magma en route to the surface (Druitt et al. 1995). The Göllüdağ and Acigöl

rhyolite fields locally feature well-preserved volcano-tectonic collapse structures interpreted as caldera ring faults (Druitt et al. 1995; Ercan et al. 1991; Mouralis et al. 2002; Türkecan et al. 2004). Two massive stratovolcanoes (Hasan Dagi, Erciyes Dagi) are constructed on older CVP volcanics (Aydar and Gourgaud 1998; Deniel et al. 1998; Kürkçüoglu et al. 1998). They represent the youngest (Holocene to historic) volcanism in the CVP, and their locations are controlled by major strike-slip and local extensional faults (Alıcı-Şen et al. 2004; Aydar and Gourgaud 1998; Bozkurt 2001; Toprak 1998; Toprak and Göncüoğlu 1993).

Mantle tomography indicates that CVP volcanism correlates with anomalously hot and thin lithosphere at depth (Al-Lazki et al. 2004; Dilek and Sandvol 2009; Gans et al. 2009; Gök et al. 2003). Modern CVP basalts are generated in the absence of ongoing subduction (seismic imaging of the upper mantle lacks evidence for the oceanic slab extending downward from the Cyprean trench; Dilek and Sandvol 2009), yet they are transitional between calc-alkaline and alkaline compositions (Alıcı-Şen et al. 2004; Aydin 2008; Deniel et al. 1998; Gencalioglu-Kuscu and Geneli 2010). This implies that their mantle source has a geochemical arc imprint that stems from a phase of previous subduction (Alıcı-Şen et al. 2004; Deniel et al. 1998; Temel et al. 1998a).

Acigöl volcanic stratigraphy and previous dating

Based on field relations and limited radiometric dating, the Acigöl complex has been identified as the eruptive center for regionally widespread Pleistocene pyroclastic fallout and flow deposits (Batum 1978; Ercan et al. 1991; Yıldırım and Özgür 1981). These deposits form an extensive veneer on the Miocene–Pliocene ignimbrites and sedimentary strata, mainly to the E and N of the Acigöl complex (Fig. 2; Druitt et al. 1995; Mouralis et al. 2002; Türkecan et al. 2004), and serve as a tephrochronologic marker horizon in distal locations (Kuzucuoglu et al. 1998; Le Pennec et al. 1994; Temel et al. 1998b). Druitt et al. (1995) separated them into Lower Acigöl Tuff (LAT), which is locally overlain by paleosol and basaltic scoria, and the Upper Acigöl Tuff (UAT). To the S of the Acigöl center, UAT drapes the flanks of a basaltic cinder cone (Armutlu Tepe), whereas to the N it is overlain by basaltic lava flows with outcrops in and around Alacaşar village.

The main part of the Acigöl complex is a rhyolite field that comprises two clusters of rhyolite domes (Fig. 2; Online Resource 1): (1) an older, morphologically subdued dome complex in the east (Boğazköy, Kocadağ, Taşkesik), and (2) a roughly N–S-oriented array of younger domes with well-preserved tuff rings in the west (from N to S: Karniyarik, Kuzey, Tepeköy, Kaleci, Güneydağ, Korudağ). Compositionally, the eastern group is slightly less evolved than the western group, with Kocadağ being distinctly less evolved than other eastern group rhyolites (Siebel et al. 2011). Boğazköy lavas are exposed along a prominent N–S-oriented scarp resulting from down-faulting during the UAT eruption (Online Resource 1; Druitt et al. 1995). Caldera morphological margins, however, are absent to the W and N and pre-date the eruption of UAT in the S (Druitt et al. 1995), possibly resulting from a fissure eruption or trapdoor caldera geometry with a N–S-oriented hinge zone. Some workers interpreted steeply dipping flow-banding in some rhyolites to indicate ring-dike intrusions surrounding major domes (Mouralis et al. 2002; Türkecan et al. 2004). We disagree with this interpretation because we have identified subhorizontal contacts between lavas and UAT (Online Resource 1). Phreatomagmatic explosion craters (e.g., the Acigöl maar) represent the youngest volcanic activity in the area and spatially coincide with the western group domes. Morphologically pristine basaltic cinder cones and a prominent N–S elongated maar crater are clearly younger than UAT as evidenced by lack of onlap or infill. The combined outflow volume of LAT and UAT is $\sim$30 km^3 (actual volume given in Druitt et al. 1995), and we estimate a dense rock equivalent of the erupted volume of $\sim$15 km^3 (density of unwelded tuff $\sim$1.3 g/cm^3 vs. magma density $\sim$2.6 g/cm^3; Lepetit et al. 2009). The combined volume of western group lava domes is $\sim$0.9 km^3, whereas eastern group volumes are difficult to estimate because they are largely covered by UAT.

Few radiometric dates exist for Acigöl. Published obsidian fission track (FT) ages agree with morphologic and stratigraphic observations, indicating younging of dome lavas from E to W (Bigazzi et al. 1993; Wagner et al. 1976), but these ages vary widely for individual sample locations. Older (eastern group) obsidians yielded FT ages of $\sim$180 to 150 ka, with the exception of Taşkesik ($\sim$75 ka; Bigazzi et al. 1993). Unspiked whole-rock K/Ar ages (160 $\pm$ 3 ka) for obsidian underlying Acigöl tuff agree broadly with FT results (Slimak et al. 2008), but are significantly younger (93 $\pm$ 2 ka; Türkecan et al. 2004) for obsidian from eastern group lavas collected in the vicinity of our BOG sampling location (Fig. 2; Table 1). Obsidian FT ages for the western group domes fall between $\sim$20 and 12 ka at stated 1σ uncertainties of $\sim$30% (Bigazzi et al. 1993). The $\sim$12 ka FT age, however, appears to be inconsistent with the oldest ^{14}C ($\sim$14 ka) and U-Th carbonate ages ($\sim$16 ka) for lake sediments in the Acigöl maar that overly rhyolitic tephra compositionally identical to western group rhyolites (Kuzucuoglu et al. 1998; Roberts et al. 2001). Basal pyroclastic deposits within the Acigöl maar are also chemically correlated with tephra in deposits of Late Pleistocene Konya lake ($\sim$100 km SW of Acigöl), where they overlie cryo-perturbed paleosols ^{14}C-

Table 1 Summary of Acigöl rhyolite sampling coordinates, petrographic and chemical characteristics, and disequilibrium-corrected (U-Th)/He eruption ages

Sample name	Rock type	Cryptocrysts	Easting	Northing	(U-Th)/He eruption age (ka)	$\pm1\sigma$ (68%) (ka)	$\pm2\sigma$ (95%) (ka)	MSWD	$n_{used}/n_{excluded}$	(U-Th)/He age excluded (Ma)
BOG	rhy. lava, nearly aphyric	pl, bt, hbl	643640	4265878	190	9	22	1.1	5/1	53
KOC	rhy. lava, weakly porphyr.	pl, qtz, hbl	641976	4266450	190	11	26	3.2	6/1	1.8
LAT	rhy. pumice, aphyric	–	654928	4274822	206	17	40	6.1	5/3	9.1, 20, 38
TAS	rhy. lava, nearly aphyric	pl, qtz, hbl	639983	4267367	147	8	18	2.2	7/1	0.2
UAT	rhy. pumice, aphyric	–	644713	4266411	163	7	17	1.1	6/2	161, 23
ALA4	rhy. pumice, aphyric	–	638599	4275440	117	4	9	0.69	8/0	–
GÜN	rhy. lava, nearly aphyric	pl, bt, hbl	635286	4266998	23.8	0.9	2.1	0.47	5/2	6.0, 52
KAL	rhy. lava, nearly aphyric	pl, bt, hbl	633302	4268695	23.2	3.0	9.7	6.6	3/4	0.04, 6.5, 6.7, 238
KAR	rhy. lava, nearly aphyric	pl, bt, hbl	636826	4276086	22.3	1.1	2.5	2.4	6/2	0.02, 73
KOR	rhy. lava, nearly aphyric	pl, bt, hbl	636012	4263853	24.9	0.9	2.1	2.7	8/1	6.3
KUZ	rhy. lava, nearly aphyric	pl, bt, hbl	636117	4271903	26.0	1.5	3.4	2.7	6/0	–
TEP	rhy. lava, nearly aphyric	pl, bt, hbl	636452	4271027	25.9	0.6	1.4	1.1	8/0	–
ACI	Obsidian clast, nearly aphyric	pl, bt, hbl	635000	4269000	20.3	0.6	0.9	2.8	10/2	0.01[a], 0.03

Geographic names of sampling locations: Boğazköy (BOG), Kocadağ (KOC), Lower Acigöl Tuff SW Ürgüp (LAT), Taşkesik (TAS), Upper Acigöl Tuff E Boğazköy (UAT), pyroclastic fallout deposit in Alaçasar (ALA-4), Güneydağ (GÜN), Kaleci (KAL), Karniyarik (KAR), Korudağ (KOR), Kuzey (KUZ), Tepeköy (TEP), Acigöl maar (ACI); alternative location names used in literature: Taşkesik = Asmadağı; Karniyarik = Susamsivrisi

Abbreviations: *rhy.* rhyolitic, *porphyr.* porphyritic, *pl* plagioclase, *qtz* quartz, *bt* biotite, *UTM* coordinates zone 36 (WGS-84), *MSWD* mean square of weighted deviates

[a] Likely not zircon

dated at ~28 ka (Kuzucuoglu et al. 1998). ^{14}C and U-Th dating, therefore, brackets the youngest rhyolite eruptions at Acigöl to ages between ~28 and ~16 ka.

Basaltic volcanism at Acigöl and in its immediate surroundings appears to be broadly contemporaneous with the rhyolite eruptions. Unspiked whole-rock K/Ar ages for basalt in the northern and eastern vicinity of Acigöl range between 618 ± 14 ka and 93 ± 10 ka (Olanca 1994; Türkecan et al. 2004). In the SE part of Acigöl, available K/Ar ages are conflicting with stratigraphic relations: a scoria cone overlain by UAT yielded ages of ~110 ka, whereas two morphologically younger scoria cones lacking UAT cover are dated between ~150 and 130 ka (Olanca 1994; Türkecan et al. 2004; Slimak et al. 2008). The youngest K/Ar age for basaltic volcanism of 32 ± 3 ka is for a cone that was partially destroyed by a phreato-magmatic explosion located S of Kocadağ (Türkecan et al. 2004).

Analytical methods

Sample collection and preparation

Samples for U-Th disequilibrium and (U-Th)/He analyses were collected from near-vertical outcrops away from contacts with overlying volcanic rocks. In order to avoid rock that could have been heated by wildfires or lightning, potentially causing He-loss (Mitchell and Reiners 2003), at least ~30 cm of exposed rock surfaces was removed prior to sampling. For samples UAT and LAT, multiple pumice clasts were combined from pyroclastic fallout deposits in distal locations, away from younger overlying volcanic deposits. The exceptions are samples ALA3 and ALA4, which were deliberately collected from paleosol and an underlying pyroclastic fallout deposit, respectively. This sequence is capped by a ~7-m-thick basaltic lava flow (Online Resource 1), and sampling was conducted to test whether zircon resetting would permit dating the emplacement of the lava flow. ALA3, however, contains mostly mafic volcanic clasts and did not yield any zircon. Whole-rock samples (typically ~5 kg) were crushed and sieved, and zircon crystals separated from the washed <250 μm size fraction by gravitational settling in heavy-liquids. Prior to mounting, crystal were treated for ~3 min in cold 40% HF to remove adherent glass. Crystals were pressed into indium (In) metal with pristine zircon prism faces ("rims") exposed at the surface for secondary ionization mass spectrometry (SIMS or ion microprobe) analysis. Selected In-mounted crystals were polished to expose inner crystal domains ("interiors"). Prior to transferring sample mounts into the ion microprobe, they were coated with a conductive layer of gold.

U-Th

U-Th isotopes in zircon were analyzed with the UCLA CAMECA ims 1270 modifying techniques from Reid et al. (1997) by simultaneously counting on mass/charge = 244 (background), 246 ($^{230}ThO^+$), 248 ($^{232}ThO^+$), and 254 ($^{238}UO^+$) in multicollection mode, which augments sample throughput by ~30% owing to reduced magnet settling and counting times. Electron-multiplier (EM) and Faraday cup (FC) detector gains were calibrated by analysis of $^{235}UO^+$ and $^{238}UO^+$ and normalizing the background-corrected ion intensities to $^{238}U/^{235}U = 137.88$ (Rosman and Taylor 1998). U/Th relative sensitivities were calibrated from analyses of zircon standard 91500 with 81.2 ppm U and 28.61 ppm Th (Wiedenbeck et al. 1995). We verified the accuracy of the relative sensitivity calibration and background corrections on AS3 secular equilibrium standard (1,099 Ma; Paces and Miller 1993), which was mounted adjacent to the unknowns. The (^{230}Th)/(^{238}U) weighted averages of AS3 analyses interspersed with the unknowns is 0.991 ± 0.005 (MSWD = 1.3; $n = 26$) and 0.994 ± 0.010 (MSWD = 0.67; $n = 11$) for two analytical sessions, consistent with secular equilibrium of AS3.

The lateral dimensions of the ion microprobe spot were ~30 μm in diameter, and craters ~5 μm deep were sputtered within a ~15-min analysis using a 60 nA $^{16}O^-$ beam. Hence, rim ages correspond to the average crystallization age of the outermost 5 μm, whereas interior crystal domain analyses laterally average over ~700 μm^2 areas. We conducted cathodoluminescence imaging of randomly

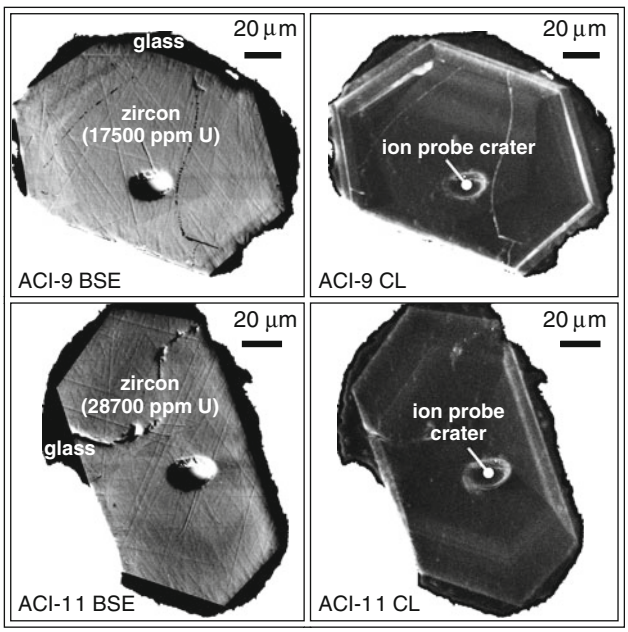

Fig. 3 Backscatter-electron (BSE) and cathodoluminescence (CL) images of selected zircon crystals from Acigöl rhyolites (sample ACI)

selected crystals and found largely homogeneous interiors so that interior ages are likely representative of a single crystallization domain (Fig. 3). Selected crystals in secular equilibrium were also dated by U–Pb ion microprobe methods (Schmitt et al. 2003).

(U-Th)/He

Following ion microprobe U-Th rim analysis, we plucked out crystals for (U-Th)/He analysis with a preference for large, euhedral, high-U, and secular equilibrium crystals because of the simplicity of corrections for alpha ejection (Ft; Farley et al. 1996) and disequilibrium (Farley et al. 2002). Crystals were photographed, measured, and transferred into niobium (Nb) tubes. (U-Th)/He dating of single crystals was performed with ^{4}He, ^{238}U, and ^{232}Th measured by quadrupole isotope-dilution mass spectrometry (MS) (for He) and inductively coupled plasma (ICP) MS (for U and Th). ^{4}He was extracted at ~1,250°C under high vacuum using a Nd-YAG laser and analyzed on the CSIRO Earth Science and Resource Engineering extraction line at the John de Laeter Centre for Isotope Research in Perth (Australia) on a Pfeiffer Prisma QMS-200 mass spectrometer. Released gas was purified using a "cold finger" cooled with liquid nitrogen and a hot (~350°C) Ti-Zr getter, spiked with 99.9% pure ^{3}He and introduced into the mass spectrometer next to a cold Ti-Zr getter. ^{4}He/^{3}He ratios were measured using a Channeltron detector operated in static mode and corrected for HD and ^{3}H interferences by monitoring mass/charge = 1 amu. A "re-extract" was run after each sample to verify complete outgassing of the crystals. He gas results were corrected for blank, determined by heating empty Nb tubes using the same procedure. After the ^{4}He measurements, Nb tubes containing the crystals were retrieved from the laser cell. Following the dissolution procedure of Evans et al. (2005), the samples were spiked with ^{233}U and ^{230}Th and dissolved in Parr bombs using HF and HCl. Sample, blank, and spiked standard solutions were analyzed for ^{238}U and ^{232}Th at TSW Analytical Ltd (University of Western Australia, Perth) on an Agilent 7500 ICP MS (Evans et al. 2005).

Analytical uncertainty of raw He ages was calculated by propagating uncertainties of U, Th, and He measurements, which was typically <5% (1σ). The raw He ages were Ft-corrected assuming a homogeneous distribution of U and Th. Since the error of the Ft correction increases with decreasing crystal size (Farley et al. 1996), values of 5% and 10% were adopted as the Ft correction uncertainties for large (Ft $\geq$ 0.65) and small crystals (Ft < 0.65), respectively.

(U-Th)/He zircon ages calculated assuming U-series equilibrium will significantly underestimate young eruption ages because deficits in the long-lived intermediate daughter isotope ^{230}Th (half-life ~75.69 ka) are common. ^{231}Pa excess (half-life ~32.76 ka), by contrast, produces He that is unsupported if radioactive equilibrium at the time of crystallization is assumed. U-series radioactive decay during pre-eruptive crystal residence reduces the degree of disequilibrium (Farley et al. 2002). To correct (U-Th)/He zircon ages for disequilibrium and crystal residence, we first constrain zircon-melt fractionation of Th and Pa relative to U (D_{230} and D_{231}, respectively; Farley et al. 2002; Schmitt et al. 2010). D_{230} is calculated from zircon Th/U divided by whole-rock Th/U (Siebel et al. 2011), and D_{231} is estimated from the published Pa/U zircon-rhyolite melt partitioning ratio of 3 (Schmitt 2007). Melt disequilibrium is reasonably neglected because continental rhyolites are typically close to secular equilibrium for ^{230}Th/^{238}U, ^{231}Pa/^{235}U, and ^{234}U/^{238}U (e.g., Pickett and Murrell 1997). Second, we apply crystallization age corrections that are based on U-Th rim analyses (eastern group, UAT, LAT), and the isochron age for crystal interiors (western group), noting that for older samples the differences between rim and interior ages are negligible relative to analytical uncertainties. Typically, seven (range 3–10) individual crystals per sample were averaged to obtain best-fit, disequilibrium-corrected eruption ages with uncertainties accounted for by Monte Carlo simulation (MCHeCalc; Schmitt et al. 2010). Scatter of (U-Th)/He zircon ages for individual samples is mostly commensurate with analytical uncertainties (as indicated by a mean square of weighted deviates [MSWD] close to unity), but for some samples elevated MSWDs indicate excess scatter. We suspect that this is caused by crystal-to-crystal age variability in excess of the interior isochron uncertainty, and/or our simplified assumptions regarding zircon crystal geometry, the distribution of parent nuclides, and the presence of inclusions affecting the accuracy of the Ft correction. Regardless of the causes of excess scatter, we accounted for it by scaling all age averages by the square root of the MSWD if >1. To simplify comparison with published geochronological data from Acigöl (Bigazzi et al. 1993), we report age uncertainties at 68.3% confidence (1σ errors; Table 1).

Results

Zircon crystallization ages

U-Th zircon ages for Acigöl rhyolite lavas and pumice fall into three categories (Figs. 4, 5, 6; Online Resource 2): (1) data on the equiline that represent xenocrysts in secular equilibrium; (2) a tight array with an approximate age of ~190 ka; these are from UAT, LAT, and eastern group rhyolites; (3) interior and rim analyses from western group rhyolites which are strongly displaced from the equiline at

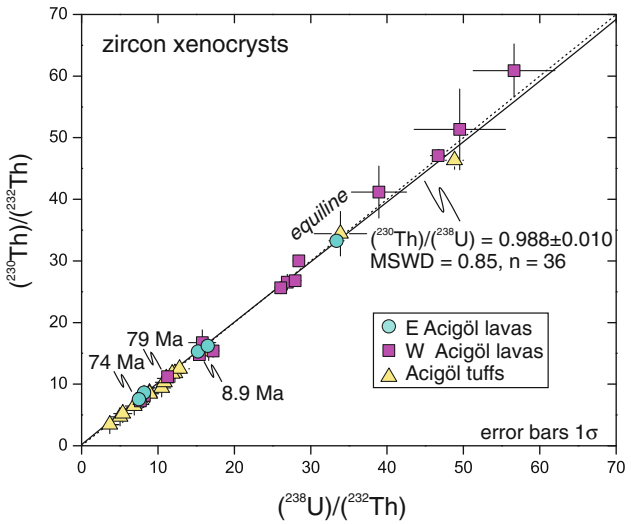

Fig. 4 ^{230}Th–^{238}U isochron diagram for xenocrystic zircon from Acigöl tuff and lava samples. Slope corresponding the (^{230}Th)/(^{238}U) is indistinguishable from unity, consistent with secular equilibrium of xenocrysts

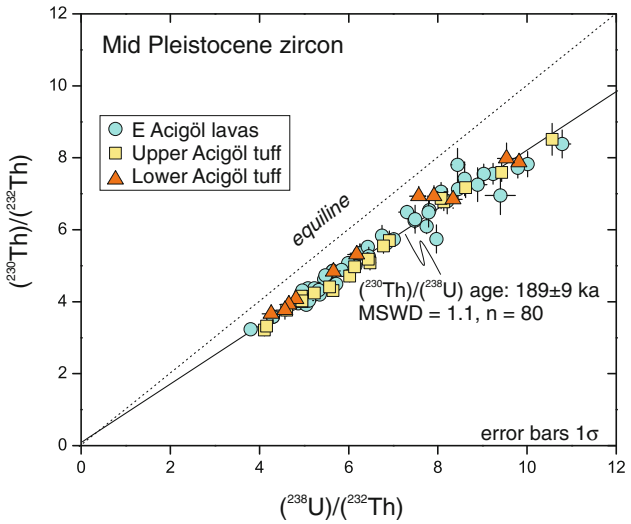

Fig. 5 ^{230}Th–^{238}U isochron diagram for Middle Pleistocene zircon from LAT, UAT and eastern Acigöl lava samples. Linear regression is consistent with a single zircon crystallization age population of ~190 ka. This is interpreted as a common magma reservoir located underneath the eastern part of Acigöl which episodically erupted over a brief time span, likely few 10's of ka indicated by (U-Th)/He zircon eruption ages

~30 to 25 ka. Reconnaissance U–Pb dating of xenocrysts (category 1) yields ^{206}Pb/^{238}U ages of ~79, 74, and 8.9 Ma (Fig. 4; Online Resource 3), confirming their old age. The linear regression slope of (^{230}Th)/(^{238}U) = 0.988 ± 0.010 (MSWD = 0.85; n = 36) for these xenocrysts is consistent with secular equilibrium and verifies the accuracy of the method. Morphologically, xenocrysts are frequently distinct from disequilibrium zircons: they show yellow-brownish color, suggesting metamictization. A

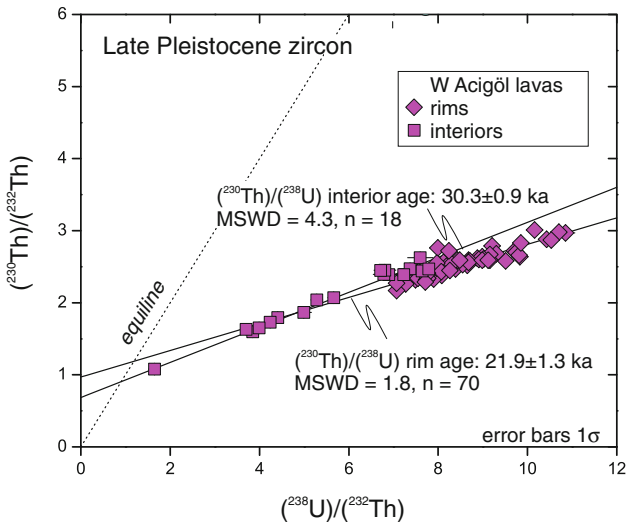

Fig. 6 ^{230}Th–^{238}U isochron diagram for Late Pleistocene zircon from western Acigöl lava dome samples and Acigöl maar ejecta clast. Separate isochrons for zircon rim and interior analyses reveal a resolvable duration of zircon crystallization corresponding to radial growth rates between 10^{-13} and 10^{-14} cm/s

regression through all category 2 zircons yields a U-Th age of 189 ± 9 ka (MSWD = 1.1; n = 80), indicating a homogenous population for this sample group (Fig. 5). This population also comprises zircon ages from additional samples of a regional intercomparison of UAT, LAT, and Kocadağ (courtesy E. Aydar; Online Resource 2) that agree with the results from our sample locations (Fig. 2). Category 3 zircons (combining rims and interiors) yield a U-Th age of 25.4 ± 0.5 ka (MSWD = 5.6; n = 88). Systematic age or compositional differences between individual samples from the western group are absent (Table 1), and therefore, this variation cannot be attributed to age heterogeneity in different parts of the Acigöl magma system. Overlapping (U-Th)/He ages lend further support to this interpretation. The high MSWD implies age heterogeneity and is reduced by separately calculating rim (21.9 ± 1.3 ka; MSWD = 1.8; n = 70) and interior isochron ages (30.3 ± 0.9 ka; MSWD = 4.3; n = 18). Rim and interior isochrons yield slightly different initial (^{230}Th)/(^{232}Th) = 1.20 ± 0.10 and 0.90 ± 0.05, respectively. These differences could indicate chemical changes in the magma system during zircon crystallization, which is also suggested by changes in zircon U abundance (lower in rims) and U/Th (higher in rims). Although the variability of rim and interior ages still exceeds the limits of the MSWD distribution at 95% confidence, this is accounted for by scaling the uncertainty by the square root of the MSWD. We thus interpret the differences between rim and interior isochron ages (and the variations within each group) as the duration of zircon crystallization that lasted for several thousand years. This is further supported by resolvable

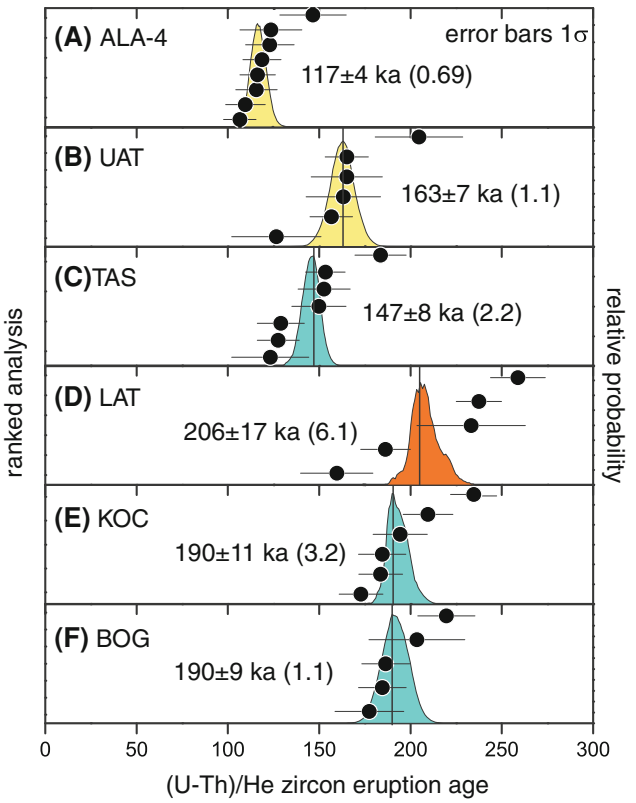

Fig. 7 Ranked disequilibrium-corrected (U-Th)/He zircon ages with probability distribution of best-fit average age for individual samples of LAT, UAT and eastern Acigöl lavas. Eruption ages, uncertainties, and MSWD values (*in parentheses*) are indicated

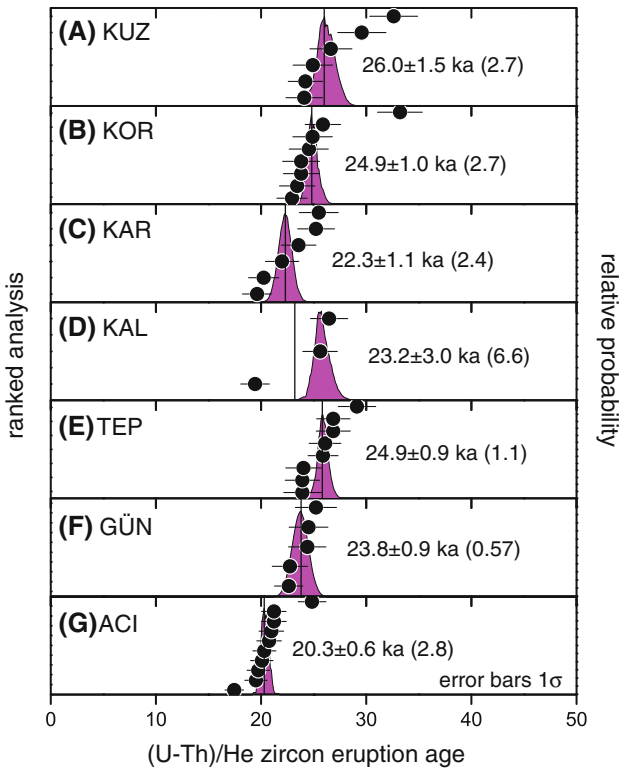

Fig. 8 Ranked disequilibrium-corrected (U-Th)/He zircon ages with probability distribution of best-fit average age for individual samples of western Acigöl lava domes and Acigöl maar ejecta clast. Eruption ages, uncertainties, and MSWD values (*in parentheses*) are indicated

differences in crystallization model ages for individual crystals (e.g., age for KAR-16 interior: 29.8 ± 0.7 ka; rim: 25.3 ± 1.1 ka), and the concordance between rim and (U-Th)/He eruption ages.

Eruption ages

(U-Th)/He zircon results mirror the dichotomy of the disequilibrium zircon crystallization ages: category 2 zircon crystals are generally much older than category 3 zircons (Figs. 7, 8; Online Resource 4). Occasionally, there are significant deviations from this pattern in some samples. Prior to describing the results in detail, it is important to recall that (U-Th)/He zircon ages in volcanic rocks represent cooling ages that in the simplest case relate to eruptive quenching or rapid cooling of lava or pyroclastic rocks at the surface. It has been demonstrated that (U-Th)/He zircon ages can be reset through partial or complete loss of ^{4}He in subsequent heating events (Blondes et al. 2007). In volcanic successions, this could be the case for heating of older rocks in contact with younger lavas or hot pyroclastic deposits. As previously stated, our sampling was targeted to avoid such rocks, with the exception of sample ALA4.

Disequilibrium-correction significantly diminishes the (U-Th)/He age dispersion of the secular equilibrium ages (Online Resource 4), and after excluding xenocrysts with pre-Pleistocene (U-Th)/He ages (described in detail at the end of this section), most replicates satisfy the goodness-of-fit criterion for a single population. Three samples with Middle Pleistocene U-Th zircon ages (LAT, Boğazköy, Kocadağ) yield tightly overlapping eruption ages between 206 ± 17 ka and 190 ± 9 ka (Fig. 7; Table 1). Unlike Druitt et al. (1995) who classified Kocadağ as an intermediate-aged dome based on younger obsidian FT ages (Bigazzi et al. 1993), we determined that it is coeval with Boğazköy (Table 1). The slightly younger (U-Th)/He zircon eruption ages for UAT and Taşkesik overlap within uncertainty at ~150 ka (Fig. 7; Table 1). Pumice from a pyroclastic fallout deposit (sample ALA4 mapped as UAT by Druitt et al. 1995) yields a distinctively younger age of 117 ± 4 ka (MSWD = 0.69; Fig. 7; Table 1). This sample was collected below the contact to an overlying basaltic lava flow. Paleosol directly at the contact was reddened indicating heating. There is ambiguity as to whether ALA4 represents a separate eruption or if it represents part of UAT thermally reset by the emplacement of the basalt. Over reasonable cooling timescales for a basaltic lava

flows (several months to years; Forman et al. 1994), significant loss of ^{4}He would only occur if temperatures reached >450°C (estimated from HeFTy modeling; Ketcham 2005). One-dimensional thermal modeling of a basalt flow heating underlying rocks suggests temperatures >400°C to within ~0.6 m below the contact (Forman et al. 1994). It thus seems unlikely that zircon resetting would have occurred ~4 m below the projected contact where ALA4 was collected (Online Resource 1). The scenario in Forman et al. (1994), however, neglects additional factors that could cause more intense heating such as convective heat transport (e.g., in water-saturated rocks), latent heat of crystallization in the basalt, and complex contact geometries (e.g., lateral heating). In the absence of better constraints on these parameters, and because whole-rock chemistry and zircon crystallization ages are identical between ALA4 and UAT sampled elsewhere, we tentatively treat the ~117 ka age as a minimum age for the eruption.

Category 3 zircons yield Late Pleistocene (U-Th)/He eruption ages that are indistinguishable between individual domes (Fig. 8; Table 1). We calculated an overall average for all domes of 24.7 ± 0.4 ka (MSWD = 2.1). Zircon extracted from an obsidian ejecta clast within Acigöl maar tuff-ring deposits is marginally younger compared to the domes (20.3 ± 0.4 ka; MSWD = 2.8; Fig. 8). Mineralogically and from its U-Th zircon crystallization ages, this clast is indistinguishable from western group dome lavas. It is therefore unresolved whether the younger age of the Acigöl maar sample represents ^{4}He-loss in an accidental lithic fragment during the maar eruption or if it originated as a hot, juvenile clast. Because of this uncertainty, we treat the 20.3 ka age as a maximum age for the Acigöl maar formation.

We have also identified several zircon xenocrysts with much older (U-Th)/He ages compared to the Pleistocene population (ranging between ~0.2 and 239 Ma; Table 1; Online Resource 4). Notably, pumice samples contain a significant proportion of xenocrysts, but they are also abundant in lava samples (e.g., Kaleci, Güneydağ). All zircons that yielded old (U-Th)/He ages were also in U-Th secular equilibrium (Online Resource 4). Some secular equilibrium crystals (e.g., TAS-12, BOG-13, LAT-10; Online Resource 4) yielded young (U-Th)/He ages overlapping those of zircon in U-Th disequilibrium. This is expected for xenocrysts reset by the magma prior to or during the eruption because outgassing occurs rapidly at magmatic temperatures (Blondes et al. 2007). By contrast, a surprisingly large number of secular equilibrium zircon crystals also yielded old (U-Th)/He ages, despite great care in the field to collect dense and uncontaminated lava at least 30 cm below the surface. We cannot estimate the degree of ^{4}He-loss in these crystals because we do not know their crystallization ages (U-Th secular equilibrium only indicates crystallization prior to ~350 ka), but we can rule out that they are true xenocrysts with protracted magmatic residence which would have led to complete outgassing.

Discussion

Late Pleistocene volcanism in Central Anatolia at high temporal resolution

Nearly identical zircon rim crystallization and eruption ages bolster confidence in the accuracy of the dating. This is fortuitous for Acigöl, whereas for many other rhyolites (e.g., Miller and Wooden 2004; Reid et al. 1997; Simon et al. 2008) zircon crystallization can significantly pre-date eruption ages which are commonly determined using conventional geochronometers (e.g., ^{40}Ar/^{39}Ar, ^{14}C). Clearly, extended periods of pre-eruptive zircon crystallization are not an artifact of intercalibration uncertainties between different geochronometers because they also have been detected by combined (U-Th)/He and U-Th zircon dating, which is fundamentally tied to the same radioactive decay system and uses the same crystals (Schmitt et al. 2010). For Acigöl, combined (U-Th)/He and U-Th zircon dating produces internally highly consistent ages that reveal two major rhyolite eruption pulses with a more pronounced temporal hiatus than previously recognized (Druitt et al. 1995). There is also a clear spatial separation between Middle and Late Pleistocene eruption centers which over time migrated from E to W. The oldest identified rhyolite eruptions at Acigöl comprise the ~190 ka eastern group of rhyolite lavas and LAT. A brief (~43 ka) hiatus separates LAT and UAT eruptions which is consistent with field observations (Druitt et al. 1995), although the (U-Th)/He zircon age difference is barely resolvable at 2σ uncertainty (±43 ka; Table 1). U-Th zircon crystallization ages are indistinguishable between LAT and UAT, suggesting that both eruptions tapped the same magma system. (U-Th)/He zircon ages for Taşkesik dome overlap with those for overlying UAT, although Türkecan et al. (2004) interpret it as a resurgent dome that intruded pyroclastic deposits. In contrast to Bigazzi et al. (1993), we find no evidence for a ~70 ka dome eruption (group 2 in Druitt et al. 1995), and (U-Th)/He as well as U-Th zircon ages cluster tightly for all rhyolites in the eastern part of the Acigöl complex. Renewed rhyolitic activity occurred much later during the Late Pleistocene and was offset several km to the west. Because the Late Pleistocene domes have indistinguishable eruption ages (within only ±400 a) and are compositionally homogeneous (Druitt et al. 1995; Siebel et al. 2011), we propose that they erupted

simultaneously from a laterally extensive dike system fed by central magma system.

Our new rhyolite chronostratigraphy also offers some indirect constraints on the timing of basaltic volcanism. Basaltic-andesitic scoria cones south of Acigöl are at least ~150 ka old because they are overlain by UAT (section Loc. 61 in Druitt et al. 1995). Published K/Ar ages of morphologically pristine cinder cones in the eastern part of Acigöl suggest emplacement shortly after the eruption of UAT (Slimak et al. 2008). In the northern part of Acigöl (near Alacaşar), a basalt flow overlies putative UAT whose (U-Th)/He zircon ages were potentially reset at or after ~117 ka. Hence, basalt flows appear to pre-date the Late Pleistocene rhyolites, which is consistent with our field observations of rhyolitic tuff ring deposits overlying basaltic lavas at Karniyarik. However, Acigöl maar sediments overlying the ~20 ka rhyolitic tephra contain exclusively basaltic tephra which suggests that at least some local basaltic vents continued to erupt after ~20 ka, whereas rhyolitic volcanism had ceased by then (Kuzucuoglu et al. 1998).

Protracted hiatuses between rhyolite eruption pulses (~125 ka between Middle and Late Pleistocene eruptions at Acigöl) have been documented elsewhere: ~200 ka intervals of quiescence separated post-caldera eruptions at Long Valley, and even longer (~300 to 500 ka) gaps exist for Early Pleistocene Coso rhyolite domes, as well as between Older and Younger Glass Mountain domes (e.g., Bailey et al. 1976; Duffield et al. 1980; Metz and Mahood 1985; Simon et al. 2009). In other cases, however, eruptive recurrence is much more frequent (~1,000 to 10,000 a), such as for the Late Pleistocene-Holocene Inyo-Mono, as well as Late Pleistocene Coso rhyolite dome complexes (Bailey et al. 1976; Duffield et al. 1980; Sieh and Bursik 1986; Simon et al. 2009). Coeval basaltic volcanism at Acigöl is typical for other rhyolite fields as well, as is the spatial distribution of basaltic vents dominantly in the periphery of the central region of rhyolite volcanism (Bacon 1985). The broadly linear alignment of the Late Pleistocene Acigöl domes conceivably indicates the opening of feeder dikes perpendicular to the least regional stress component which is approximately E–W-oriented (Toprak 1998; Toprak and Göncüoğlu 1993). The overall duration of bimodal magmatism at Acigöl is therefore similar to other intra-continental rhyolite fields, but more "hyperactive" centers also exist where rhyolite eruptions occur more frequently. Prior to interpreting these relations, it is important to first consider additional evidence from zircon crystallization ages.

Zircon growth rates: observations, kinetics, and thermal models

High-resolution zircon geochronology is important for tracking the pre-eruptive melt evolution, but for older rhyolite fields preserved in the geologic record (e.g., Duffield and Dalrymple 1990) the temporal resolution is insufficient to reveal crystallization and crystal residence time-scales at submillennial resolution. Because of the young age of Acigöl rhyolites and the unrivaled spatial selectivity of ion microprobe analysis, we have the rare ability to quantify the duration of zircon crystallization. By using the difference between interior and rim crystallization ages, or to the same effect the (U-Th)/He eruption ages, we can constrain the duration of pre-eruptive zircon crystallization to ~6 to 8 ka for Late Pleistocene Acigöl rhyolites, with uncertainties of ~2 ka. For a typical ~50-μm-radius zircon, this translates into radial growth rates of $\sim 3 \times 10^{-14}$ cm/s, assuming that zircon continuously crystallized between nucleation and rim growth (eruption). These growth rates overlap the upper range of zircon crystallization rates (10^{-13}–10^{-17} cm/s; Watson 1996) from a kinetic model that is based on experimental diffusion data at temperatures equivalent to those indicated by zircon saturation for Acigöl (T_{sat} = 795–741°C; Druitt et al. 1995; Siebel et al. 2011). This overlap (at order-of-magnitude resolution) seems reasonable when accounting for uncertainties in zirconium diffusion parameters (e.g., temperature, water abundance; Harrison and Watson 1983). Moreover, processes such as convection or shearing could accelerate zircon crystallization beyond diffusion-limited growth (Watson 1996).

Although kinetically plausible, the brief zircon crystallization durations at Acigöl are atypical for many small-volume rhyolites (Simon et al. 2008). We, therefore, also explore thermal models to compare observed zircon crystallization time-scales to those expected from heat balance calculations taking into account sensible and latent heat released during the crystallization of magma, and heat transport through the wall-rocks surrounding a cooling magma body. For this, we adopt the crystallization scale-time parameterization of Fowler and Spera (2010) for the duration of magmatic heat loss in relation to the erupted volume of differentiated magma $V_{erupted}$ and heat flow q:

$$\tau = \frac{\rho \Delta H}{Kq} \sqrt[3]{\frac{V_{erupted}}{\alpha f}} \quad (1)$$

with additional variables f = fraction of melt remaining at eruption, α = fraction of erupted melt, K = geometry parameter (between 5 and 7 for cubical, spherical, or slab-like magma bodies), and ΔH the magma enthalpy difference between its liquidus and eruption temperatures. To calculate a model zircon crystallization time t_z, τ is multiplied by a factor:

$$t_z = \tau(1 - f_{H,sat}) \quad (2)$$

with $f_{H,\,sat}$ defined as the fractional enthalpy loss between the liquidus (~1,150°C) and the modeled zircon saturation

temperature relative to the total enthalpy released by the magma up to the eruption temperature (~750°C estimated from the actual zircon saturation temperature). We estimated $f_{H,\ sat} = 0.8$ from applying the zircon saturation model to melt compositions predicted by MELTS (Asimow and Ghiorso 1998; Ghiorso and Sack 1995) taking a Quaternary basalt of the Acigöl complex with Zr = 150 ppm (Siebel et al. 2011) as the starting composition and assuming that Zr is incompatible in all phases (mineral–melt partitioning $D = 0$) except zircon. For the MELTS simulation (170 MPa isobaric, fixed fO_2 = QFM + 2) and crystallization time-scale calculations ($\rho = 2{,}150$ kg/m^3; $K = 5$; $\Delta H = 0.87$ MJ/kg), we used values similar to those in Fowler and Spera (2010) for Bishop Tuff high-silica rhyolite whose eruptive temperatures and chemical signatures (low-Sr, low-Ba) are similar to Acigöl rhyolites. In the absence of better constraints, all calculations assumed a value of $\alpha = 1$, which represents a lower bound for the crystallization time. Although MELTS has limitations in modeling hydrous rhyolitic compositions, we note that conditions for zircon saturation estimated using MELTS for a basaltic composition are reasonably close to those based on experimental glass data for an intermediate starting composition (Harrison et al. 2007): $T_{sat} = 880$°C vs. 830°C, and $f = 0.3$ vs. 0.45, respectively. The heat flow parameter q in Eq. 1 is poorly known. An absolute lower limit is set by amagmatic continental crustal heat flow (0.065 mW/m^2), whereas the upper limit is estimated from heat flow in hydrothermally active regions associated with continental hot spots (e.g., Yellowstone 2 W/m^2; Fowler and Spera 2010). Within this wide range for q, we expect to enclose global conditions for magmatic heat loss in continental environments. Minor crustal assimilation (Siebel et al. 2011) will have a compensatory effect on zircon crystallization timescales because the faster enthalpy loss through melting of country rock will be offset by an earlier onset of zircon saturation because of addition of excess Si and Al. Because of the overall uncertainties in this model and its simplifications regarding many real-world complexities (e.g., non-idealized geometry, open-system processes), we emphasize that its purpose is not to realistically constrain magma chamber cooling, but rather to estimate reasonable zircon crystallization durations as a function of magmatic heat loss and magma volume at order-of-magnitude resolution.

Model curves for different q values delineate three major fields: in the upper-left segment of Fig. 9, crystallization durations exceed even the slowest cooling rates permitted by amagmatic heat flow. In the lower-right segment, zircon crystallization time-scales are too short compared to the modeled onset of zircon saturation even for extremely rapid heat dissipation. The region bracketed by these bounding heat flow curves is broadly permissive

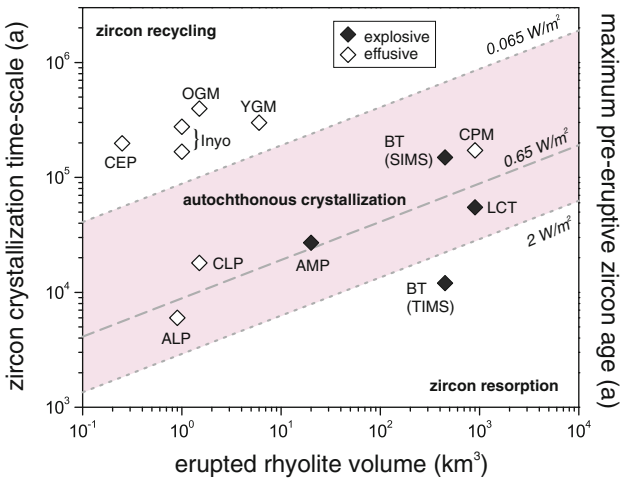

Fig. 9 Modeled zircon crystallization time-scales vs. volume of erupted rhyolite magma. Pre-eruptive zircon crystallization ages for Middle and Late Pleistocene Acigöl rhyolite eruptions (AMP and ALP, respectively) and selected intra-continental rhyolite fields from the western USA are based on difference between eruption age and the oldest zircon dated. Data compiled from Simon et al. (2008), Simon et al. (2009), and Crowley et al. (2007), with erupted volumes estimated as estimated dense rock equivalents and plotted on same ordinate scale. AMP, ALP, and Late Pleistocene Coso (CLP) zircon ages fall within model limits for autochthonous crystallization (i.e., within the same magma that erupts after some degree of fractional crystallization), as do many large-volume systems (Yellowstone Lava Creek Tuff LCT and Central Plateau Member flows CPM, as well as Bishop Tuff BT). By contrast, zircon antecrysts in many small-volume systems (Early Pleistocene Coso CEP, Inyo, Younger Glass Mountain YGM and Older Glass Mountain OGM) are too old for single-stage magma cooling under reasonable heat flow conditions (*upper left field*). Preponderance of excessively old antecrysts could indicate zircon recycling from a voluminous intrusive complex or from a long-lived crystal mush. Zircon resorption is a potential mechanism to rid rhyolites of antecrysts (*lower right field*), but the BT case remains inconclusive because contrasting estimates for pre-eruptive zircon crystallization time-scales have been obtained using different analysis techniques (see text). Note that the upper limit (average continental heat flow) is unrealistic for the right-hand side of the diagram (i.e., large magma volumes)

for "autochthonous" zircon crystallization, i.e., in a single batch of magma undergoing cooling and differentiation with rates permitted by heat flow constraints. We compare these fields with the observed zircon crystallization time-scales estimated from the difference between the oldest antecryst (Miller et al. 2007) in a sampled zircon population and the eruption age (Fig. 9). Zircon data for many continental rhyolite systems fall within the bounds consistent with autochthonous crystallization, including Acigöl. Equation 2 can also be used to estimate the duration of basalt-rhyolite differentiation; for example, using $t_z = 6$ ka for Late Pleistocene Acigöl zircons, the onset of basalt differentiation would have occurred ~30 ka prior to eruption.

We emphasize that this model is not proof of closed-system, single-batch magma differentiation at Acigöl or

any other system plotted in Fig. 9. In fact, it is more instructive to consider pre-eruptive zircon ages that fall outside the modeled bounds: many small-volume rhyolites host zircon antecrysts that are much older than expected given their small erupted volumes (those plotting in the upper-left segment in Fig. 9). Few exceptions exist to this pattern for continental rhyolite fields: besides Acigöl, we are only aware of Late Pleistocene Coso rhyolites having U-Th zircon (and allanite) ages that are within uncertainty of the $^{40}Ar/^{39}Ar$ eruption age (Simon et al. 2009). Because of the small number of Late Pleistocene Coso zircons analyzed, their statistical relevance is somewhat uncertain because it cannot be ruled out that older antecrysts were overlooked. This, however, seems unlikely for Acigöl with more than 200 zircons analyzed. Abundant zircon antecrysts in small-volume eruptions could indicate recycling from zircon-bearing plutonic predecessors via re-melting and assimilation (Bacon and Lowenstern 2005; Lowenstern et al. 2000; Schmitt et al. 2003), versus protracted crystallization in partial melt pockets in long-lived crystal mushes (Bachmann and Bergantz 2004; 2008). These two scenarios could be distinguished by discontinuous vs. continuous zircon crystallization. Our zircon growth rates predict that zircon rims should develop thicknesses sufficiently thick ($\sim$µm over 1,000 years at $\sim$750°C) to be detectable by ion microprobe depth profiling. Regardless of continuous vs. discontinuous melt presence within the magmatic plumbing system, evidence of excessively old zircon antecrysts in many systems (but not Acigöl) implies that intrusive volumes are more extensive than indicated by extrusive volumes.

The only other case where zircon crystallization ages fall clearly outside the thermal model bounds is Bishop Tuff. Here, TIMS zircon crystallization ages (Crowley et al. 2007) plot below the model curve for rapid heat loss (lower-right segment in Fig. 9), whereas maximum ages of crystal interiors analyzed by SIMS are well within limits (Simon and Reid 2005; Simon et al. 2008). We will not further explore potential geologic implications of this observation because of unresolved issues regarding the reliability of TIMS analysis in constraining the onset of zircon crystallization. This is because the symbols plotted in Fig. 9 are minimum estimates, where antecrysts may have gone undetected if only a comparatively small number of crystals were analyzed (19 in Crowley et al. 2007 vs. 53 in Simon and Reid 2005 and references therein). Moreover, bulk analysis by TIMS is expected to be biased toward high-U crystal rims, which potentially masks the presence of early-crystallized low-U cores.

An important question bearing on the reliability of the zircon record, however, remains: if zircon crystallization durations are lower than expected (as is the case for Acigöl in comparison with many other small-volume systems), could zircon antecrysts have been somehow lost prior to eruption? Assuming that the Late Pleistocene eruptions at Acigöl were in fact fed from a voluminous and long-lived magma body at depth, we explore potential mechanisms for ridding rhyolite melts of zircon antecrysts. Settling of individual zircon crystals can be ruled out because it is exceedingly slow in viscous rhyolites (Reid et al. 1997). If zircon was an inclusion in a dense, larger crystal (e.g., Fe–Ti oxide), it could settle faster, but we deem this implausible because of the petrographic observation that zircon is matrix-hosted and in mineral separates ubiquitously has adherent glass, implying that the crystals were suspended in the melt. For the same reason, whole-sale downward transport of zircon trapped in crystal-rich domains within the magma reservoir seems unlikely. Thermal resorption of zircon is prohibited under conditions of isothermal or retrograde melt residence. The period of eruptive quiescence between the Middle and Late Pleistocene rhyolite eruption pulses would be sufficient to resorb zircon if the magma had heated up and became strongly undersaturated (Harrison and Watson 1983; Watson 1996). This, however, seems implausible because the Late Pleistocene rhyolites indicate cooler and chemically more-evolved magma conditions relative to their Middle Pleistocene precursors (e.g., zircon saturation temperatures decreasing from 795–762°C to 745–741°C with time; Siebel et al. 2011). We cannot rule out the possibility that cooling and differentiation followed zircon resorption during transient heating, but such a scenario would involve significant addition of juvenile basaltic magma to the system, thermally equivalent to our model of basalt differentiation.

Hence, zircon loss via crystal settling or resorption is unrealistic for rhyolitic magma systems undergoing monotonic cooling, and a poor explanation for the absence of zircon antecrysts in Acigöl rhyolites. Instead, brief zircon crystallization intervals are in agreement with model predictions for cooling of small-volume magmas under conditions of heat dissipation that are $\sim$10-times the continental average (Fig. 9). Thus, our preferred scenario is that the Middle and Late Pleistocene rhyolite pulses involved separate magmas. This is in contrast to apparent magmatic consanguinity based on chemical and thermal trends from hotter, less evolved to cooler, more-evolved rhyolites that are suggestive of a direct genetic lineage via fractional crystallization (cf. Vazquez and Reid 2002). Separate zircon crystallization pulses rule out rhyolite extraction from a voluminous and long-lived crystal mush zone where differentiated melt persisted under zircon-saturated conditions. The scarcity of true magmatic zircon xenocrysts (if any) also suggests that parental magmas initially were zircon undersaturated. In fact, most (but not all) zircon crystals in secular equilibrium escaped magmatic heating because of their old (U-Th)/He ages, and

likely were entrained during the eruption process. They can therefore be discarded as magmatic xenocrysts. In our companion paper (Siebel et al. 2011), we present further evidence that rhyolite progenitors started out as mafic magmas based on distinctively higher whole-rock εNd, and lower zircon $\delta^{18}O$ compared to potential crustal source rocks.

Patterns of bimodal volcanism in intra-continental settings

Protracted melt presence underneath intra-continental rhyolite fields and caldera-systems has important implications for crustal dynamics, volcanic hazards, and geothermal exploration. We can now refine some of the conclusions in Druitt et al. (1995) regarding the possibility of a large magma body underlying the Acigöl rhyolite field. Druitt et al. (1995) postulated a "basaltic shadow zone" (based on the absence of any basaltic vents in the region enclosed by Middle to Late Pleistocene rhyolite domes) to represent a low-density reservoir of silicic magma, or hot intrusives. However, the well-resolved hiatus (~125 ka) between rhyolite eruptions and rapid zircon crystallization time-scales (~10^3–10^4 a; Fig. 9) weakens arguments in favor of a persistent subterranean magma chamber. By the same token, we argue that the distribution of rhyolite domes is more regular than previously thought and that a clear-cut distinction exists between Middle and Late Pleistocene eruptive centers that shifted focus from E to W. Dike eruption of the broadly N–S orientated Late Pleistocene domes is consistent with regional crustal stresses indicated by basaltic vent alignments (Gautier et al. 2008; Toprak 1998; Toprak and Göncüoğlu 1993) and contrasts with diffuse silicic vent clusters in other systems that are indicative of large magma bodies at depth (Bacon 1985).

Bimodal volcanism is a hallmark of rhyolite fields such as Acigöl, but why high-silica magma is generated in some areas of basaltic volcanism and not in others remains speculative. On a regional scale, Acigöl is non-unique in that the Early Pleistocene Gölludağ rhyolite field exists only ~50 km to the south. Both fields are conjoined by a series of monogenetic cinder cones (Fig. 2). Other regional basaltic monogenetic fields that have developed over the hot and thin central Anatolian lithosphere (Dilek and Sandvol 2009) have not generated rhyolite eruptions (e.g., Karapinar; Keller 1976), whereas Holocene stratovolcanic centers (e.g., Hasan Dağı, Erciyes Dağı) are dominated by intermediate magma compositions (Alıcı-Şen et al. 2004; Aydar and Gourgaud 1998; Deniel et al. 1998; Kürkçüoglu et al. 1998). Such contrasting patterns in continental bimodal volcanism are not unusual: in eastern California, the Coso field is dominated by rhyolite (Bacon et al. 1981; Duffield et al. 1980), whereas ~100 km to the north at Big Pine (in a broadly similar tectonic setting, and approximately coeval) only one rhyolite dome erupted during the earliest stages of an otherwise basaltic volcanic field (Blondes et al. 2007; Lidzbarski et al. 2007). Conceivably, the crust beneath fields capable of producing rhyolites was thermally and compositionally pre-conditioned during phases of earlier magmatism (e.g., the presence of late Miocene calderas in the case of the Acigöl and Göllüdağ fields; Batum 1978; Froger et al. 1998; Le Pennec et al. 1994; Yıldırım and Özgür 1981), facilitating minor partial melting of mid- to shallow-crustal rocks, followed by stalling and differentiation of basaltic magmas. Once an intra-crustal hot zone is established, its localization may be self-enforcing until the underlying heat source of mantle-derived basaltic magmatism terminates.

Conclusions and outlook

The Acigöl rhyolite field is ideal for studying time-scales of rhyolite genesis and pre-eruptive magma storage because of its young age, excellent preservation owing to the absence of large explosive eruptions, and accessibility of unweathered outcrops in a semi-arid climate. By applying combined U-Th and (U-Th)/He zircon dating, consistent eruption and pre-eruptive crystallization ages were obtained which indicate two major pulses of rhyolite volcanism during the Middle and Late Pleistocene (~200 to 150 ka and ~25 to 20 ka). Zircon crystallization ages show no evidence for crystal carryover from the older to the younger pulse, despite major and trace element compositional trends suggestive of protracted fractional crystallization of a single magma body. Although zircon antecrysts predating the eruption by 10's–100's of ka abound in many rhyolite fields worldwide (e.g., Miller and Wooden 2004; Reid et al. 1997; Simon et al. 2008), they are conspicuously absent in Acigöl rhyolites. Measured radial growth rates between ~10^{-13} and 10^{-14} cm/s for Late Pleistocene Acigöl zircon are consistent with thermal models for rhyolite differentiation via fractional crystallization of small-volume basaltic parents. Acigöl thus exemplifies an intra-continental rhyolite field where coeval vents are more regularly distributed than previously known, consistent with a common feeder dike for Late Pleistocene rhyolite eruptions. Its magmatic history is characterized by episodic thermal rejuvenation that created individual, spatially segregated magmatic centers, or erased the crystal memory in more extensive pre-existing magma reservoir. For this, we favor basaltic recharge followed by rapid differentiation with minor crustal assimilation. This is in contrast to other systems where evolved melts are sequentially tapped from a long-lived crystal mush (cf. Vazquez and Reid 2002). In our companion

paper (Siebel et al. 2011), the processes of rhyolite magma generation in a bimodal system are further detailed by using a combination of whole-rock and accessory mineral isotope geochemistry.

Acknowledgments We thank Felix Wicke for photographic documentation of fieldwork, Simone Jahn for assistance in zircon separation, as well as Cam Scadding and Allen Thomas at TSW Analytical, Perth, for assistance with ICP MS. Erkan Aydar and Vedat Toprak are thanked for insightful discussions during a field trip to the area. Erkan Aydar also provided samples for the regional comparison, and Lütfiye Akın is thanked for additional zircon sample preparation. Constructive reviews by Calvin Miller and Jonathan Miller are acknowledged. We thank Jochen Hoefs for editorial handling. This study was supported by a grant from the German Science Foundation (Si 718/9-1). The ion microprobe facility at UCLA is partly supported by a grant from the Instrumentation and Facilities Program, Division of Earth Sciences, National Science Foundation.

References

Alıcı-Şen P, Temel A, Gourgaud A, Kieffer G, Gundogdu MN (2004) Petrology and geochemistry of potassic rocks in the Golcuk area (Isparta, SW Turkey): genesis of enriched alkaline magmas. J Volcanol Geotherm Res 85(1–4):423–446

Al-Lazki AI, Sandvol E, Seber D, Barazangi M, Turkelli N, Mohamad R (2004) Pn tomographic imaging of mantle lid velocity and anisotropy at the junction of the Arabian, Eurasian and African plates. Geophys J Int 158(3):1024–1040

Annen C (2009) From plutons to magma chambers: thermal constraints on the accumulation of eruptible silicic magma in the upper crust. Earth Planet Sci Lett 284(3–4):409–416

Asimow PD, Ghiorso MS (1998) Algorithmic modifications extending MELTS to calculate subsolidus phase relations. Am Mineral 83(9–10):1127–1132

Aydar E (1997) Volcanological and petrological characteristics of Karatas volcanites, Central Anatolia. Hacettepe Univ Earthsci 19:41–55 (in Turkish with English abstract)

Aydar E, Gourgaud A (1998) The geology of Mount Hasan stratovolcano, central Anatolia, Turkey. J Volcanol Geotherm Res 85(1–4):129–152

Aydin F (2008) Contrasting complexities in the evolution of calc-alkaline and alkaline melts of the Nigde volcanic rocks, Turkey: textural, mineral chemical and geochemical evidence. Eur J Mineral 20(1):101–118

Bachmann O, Bergantz GW (2004) On the origin of crystal-poor rhyolites: extracted from batholithic crystal mushes. J Petrol 45(8):1565–1582

Bachmann O, Bergantz GW (2008) Rhyolites and their source mushes across tectonic settings. J Petrol 49(12):2277–2285

Bacon CR (1985) Implications of silicic vent patterns for the presence of large crustal magma chambers. J Geophys Res Solid Earth Planets 90(NB13):1243–1252

Bacon CR, Lowenstern JB (2005) Late Pleistocene granodiorite source for recycled zircon and phenocrysts in rhyodacite lava at Crater Lake, Oregon. Earth Planet Sci Lett 233(3–4):277–293

Bacon CR, Macdonald R, Smith RL, Baedecker PA (1981) Pleistocene high-silica rhyolites of the Coso volcanic field, Inyo County, California. J Geophys Res 86(NB11):223–241

Bailey RA, Dalrymple GB, Lanphere MA (1976) Volcanism, structure, and geochronology of Long-Valley caldera, Mono-County, California. J Geophys Res 81(5):725–744

Batum I (1978) Geology and petrography of Acigöl and Göllüdag volcanic at southwest of Nevsehir Central Anatolia, Turkey. Yerbilimleri 4(1–2):50–69 (in Turkish with English abstract)

Beekman PH (1966) The Pliocene and Quaternary volcanism in the Hasan Dag-Melendiz Dag region. Bull Mineral Res Explor Inst Ankara 66:588–595

Bigazzi G, Yegingil Z, Ercan T, Oddone M, Ozdogan M (1993) Fission-track dating obsidians in Central and Northern Anatolia. Bull Volcanol 55(8):588–595

Bindeman IN, Valley JW, Wooden JL, Persing HM (2001) Post-caldera volcanism; in situ measurement of U-Pb age and oxygen isotope ratio in Pleistocene zircons from Yellowstone Caldera. Earth Planet Sci Lett 189(3–4):197–206

Blondes MS, Reiners PW, Edwards BR, Biscontini A (2007) Dating young basalt eruptions by (U-Th)/He on xenolithic zircons. Geology 35(1):17–20

Bozkurt E (2001) Neotectonics of Turkey—a synthesis. Geodinam Acta 14(1–3):3–30

Crowley JL, Schoene B, Bowring SA (2007) U–Pb dating of zircon in the Bishop Tuff at the millennial scale. Geology 35(12): 1123–1126

Deniel C, Aydar E, Gourgaud A (1998) The Hasan Dagi stratovolcano (Central Anatolia, Turkey): evolution from calc-alkaline to alkaline magmatism in a collision zone. J Volcanol Geotherm Res 87(1–4):275–302

Dhont D, Chorowicz J, Yurur T, Froger JL, Kose O, Gundogdu N (1998) Emplacement of volcanic vents and geodynamics of Central Anatolia, Turkey. J Volcanol Geotherm Res 85(1–4): 33–54

Dilek Y, Sandvol EA (2009) Seismic structure, crustal architecture and tectonic evolution of the Anatolian-African Plate boundary and the Cenozoic orogenic belts in the eastern Mediterranean region. Geol Soc Spec Publ 327:127–160

Dirik K, Göncüoğlu MC (1996) Neotectonic characteristics of central Anatolia. Int Geol Rev 38:807–817

Druitt TH, Brenchley PJ, Gokten YE, Francaviglia V (1995) Late Quaternary rhyolitic eruptions from the Acigol complex, Central Turkey. J Geol Soc 152:655–667

Duffield WA, Dalrymple GB (1990) The Taylor Creek Rhyolite of New-Mexico—a rapidly emplaced field of lava domes and flows. Bull Volcanol 52(6):475–487

Duffield WA, Bacon CR, Dalrymple GB (1980) Late Cenozoic volcanism, geochronology, and structure of the Coso-Range, Inyo-County, California. J Geophys Res 85(NB5):2381–2404

Ercan T, Yıldırım T, Akbaşlı A (1987) Gelveri (Nigde)—Kizilcin (Nevsehir) arasındaki volkanizmanın özellikleri. Jeomorfoloji Dergisi 15:27–36

Ercan T, Akbaşlı A, Yıldırım T, Fişekçi A, Selvi Y, Ölmez M, Can B (1991) Acıgöl (Nevşehir) yöresindeki senozoyik yaşlı volkanik kayaçların petrolojisi. Maden Tetkik ve Arama Dergisi 113:31–44 (in Turkish with English abstract)

Ercan T, Tokel S, Matsuda JI, Notsu K, Fujitani T (1992) New geochemical, isotopic and radiometric data of the Quaternary volcanism of Hasandağı-Karacadağ (Central Anatolia). TJK Bülteni 7:8–21 (in Turkish with English abstract)

Evans NJ, Byrne JP, Keegan JT, Dotter LE (2005) Determination of uranium and thorium in zircon, apatite, and fluorite: application to laser (U-Th)/He thermochronology. J Anal Chem 60(12):1159–1165

Farley KA, Wolf RA, Silver LT (1996) The effects of long alpha-stopping distances on (U-Th)/He ages. Geochim Cosmochim Acta 60(21):4223–4229

Farley KA, Kohn BP, Pillans B (2002) The effects of secular disequilibrium on (U-Th)/He systematics and dating of Quaternary volcanic zircon and apatite. Earth Planet Sci Lett 201(1):117–125

Forman SL, Pierson J, Smith RP, Hackett WR, Valentine G (1994) Assessing the accuracy of thermoluminescence for dating baked sediments beneath late quaternary lava flows, Snake River Plain, Idaho. J Geophys Res 99(B8):15569–515576

Fowler SJ, Spera FJ (2010) A metamodel for crustal magmatism: phase equilibria of giant ignimbrites. J Petrol 51(9):1783–1830

Froger JL, Lenat JF, Chorowicz J, Le Pennec JL, Bourdier JL, Kose O, Zimitoglu O, Gundogdu NM, Gourgaud A (1998) Hidden calderas evidenced by multisource geophysical data; example of Cappadocian calderas, central Anatolia. J Volcanol Geotherm Res 85(1–4):99–128

Gans CR, Beck SL, Zandt G, Biryol CB, Ozacar AA (2009) Detecting the limit of slab break-off in central Turkey: new high-resolution Pn tomography results. Geophys J Int 179(3):1566–1572

Gautier P, Bozkurt E, Bosse V, Hallot E, Dirik K (2008) Coeval extensional shearing and lateral underflow during late cretaceous core complex development in the Nigde Massif, Central Anatolia, Turkey. Tectonics 27(1):TC1003 1–27

Gencalioglu-Kuscu G, Geneli F (2010) Review of post-collisional volcanism in the Central Anatolian Volcanic Province (Turkey), with special reference to the Tepekoy Volcanic Complex. Int J Earth Sci 99:593–621

Ghiorso MS, Sack RO (1995) Chemical mass transfer in magmatic processes; IV, A revised and internally consistent thermodynamic model for the interpolation and extrapolation of liquid-solid equilibria in magmatic systems at elevated temperatures and pressures. Contrib Mineral Petrol 119(2–3):197–212

Gök R, Sandvol E, Turkelli N, Seber D, Barazangi M (2003) Sn attenuation in the Anatolian and Iranian plateau and surrounding regions. Geophys Res Lett 30(24). doi:10.1029/2003GL018020

Göncüoğlu MC (1986) Geochronological data from the southern part (Nigde area) of the Central Anatolian Massif. Bull Mineral Res Explor Inst (MTA) Ankara 105–106:83–96

Göncüoğlu MC, Toprak V (1992) Neogene and Quaternary volcanism of central Anatolia: a volcano-structural evaluation. Bull Sec Volcanol Soc Geol France 26:1–6

Harrison TM, Watson EB (1983) Kinetics of zircon dissolution and zirconium diffusion in granitic melts of variable water-content. Contrib Mineral Petrol 84(1):66–72

Harrison TM, Aikman AK, Watson EB (2007) Temperature spectra of zircon crystallization in plutonic rocks. Geology 35(7):635–638

Innocenti F, Mazzuoli R, Pasquarè G, Radicatidibrozolo F, Villari L (1975) Neogene calcalkaline volcanism of Central Anatolia—geochronological data on Kayseri-Nigde Area. Geol Mag 112(4):349–360

Keller J (1976) Quaternary maar volcanism near Karapinar in central Anatolia. Bull Volcanol 38(1):378–396

Ketcham RA (2005) Forward and inverse modeling of low-temperature thermochronometry data. In: Low-temperature thermochronology: techniques, interpretations, and applications, vol 58, pp 275–314

Kürkçüoglu B, Sen E, Aydar E, Gourgaud A, Gundogdu N (1998) Geochemical approach to magmatic evolution of Mt Erciyes stratovolcano central Anatolia, Turkey. J Volcanol Geotherm Res 85(1–4):473–494

Kuzucuoglu C, Pastre JF, Black S, Ercan T, Fontugne M, Guillou H, Hatte C, Karabiyikoglu M, Orth P, Turkecan A (1998) Identification and dating of tephra layers from Quaternary sedimentary sequences of Inner Anatolia, Turkey. J Volcanol Geotherm Res 85(1–4):153–172

Le Pennec JL, Bourdier JL, Froger JL, Temel A, Camus G, Gourgaud A (1994) Neogene ignimbrites of the Nevsehir Plateau (Central Turkey)—stratigraphy, distribution and source constraints. J Volcanol Geotherm Res 63(1–2):59–87

Le Pennec JL, Temel A, Froger JL, Sen S, Gourgaud A, Bourdier JL (2005) Stratigraphy and age of the Cappadocia ignimbrites, Turkey: reconciling field constraints with paleontologic, radiochronologic, geochemical and paleomagnetic data. J Volcanol Geotherm Res 141(1–2):45–64

Lepetit P, Viereck-Goette L, Schumacher R, Mues-Schumacher U, Abratis M (2009) Parameters controlling the density of welded ignimbrites—a case study on the Incesu Ignimbrite, Cappadocia, Central Anatolia. Chem Erde Geochem 69(4):341–357

Lidzbarski MI, Vazquez JA, Woolford JM, Anonymous (2007) Rhyolite magmatism in the Big Pine volcanic field, eastern California. Bull South Calif Acad Sci 106(2):107

Lowenstern JB, Persing HM, Wooden JL, Lanphere M, Donnelly-Nolan J, Grove TL (2000) U-Th dating of single zircons from young granitoid xenoliths: new tools for understanding volcanic processes. Earth Planet Sci Lett 183(1–2):291–302

Metz JM, Mahood GA (1985) Precursors to the Bishop Tuff eruption—Glass Mountain, Long Valley, California. J Geophys Res Solid Earth Planets 90(NB13):1121–1126

Miller JS, Wooden JL (2004) Residence, resorption and recycling of zircons in Devils Kitchen rhyolite, Coso Volcanic field, California. J Petrol 45(11):2155–2170

Miller JS, Matzel JEP, Miller CF, Burgess SD, Miller RB (2007) Zircon growth and recycling during the assembly of large, composite arc plutons. J Volcanol Geotherm Res 167(1–4):282–299

Mitchell SG, Reiners PW (2003) Influence of wildfires on apatite and zircon (U-Th)/He ages. Geology 31(12):1025–1028

Mouralis D, Pastre JF, Kuzucuoglu C, Turkecan A, Atici Y, Slimak L, Guillou H, Kunesch S (2002) Les complexes volcaniques rhyolitiques quaternarires D'Anatolie centrale (Göllü Dag et Acigöl, Turquie): genese, instability, contraintes environnementales. Quaternaire 13(3–4):219–228

MTA (2005) Kayseri (K33d3, d4). In: Geological Maps of Turkey, vol. Maden Tetkik ve Arama Genel Müdürlüğü (General Directorate of Mineral Research and Exploration), Ankara

Mues-Schumacher U, Schumacher R, Viereck-Goette LG, Lepetit P (2004) Areal distribution and bulk rock density variations of the welded Incesu Ignimbrite, central Anatolia, Turkey. Turkish J Earth Sci 13(3):249–267

Olanca K (1994) Geochimie des laves quaternaries de Cappadoce (Turquie). Les appareils monogéniques. In vol PhD Université Blasie Pascal, Clermont Ferrand, p 156

Paces JB, Miller JD (1993) Precise U-Pb ages of duluth complex and related mafic intrusions, northeastern Minnesota—geochronological insights to physical, petrogenetic, paleomagnetic, and tectonomagmatic processes associated with the 1.1 Ga midcontinent rift system. J Geophys Res Solid Earth 98(B8):13997–14013

Pasquarè G, Poli S, Vezzoli L, Zanchi A (1988) Continental arc volcanism and tectonic setting in Central Anatolia, Turkey. Tectonophysics 146(1–4):217–230

Pickett DA, Murrell MT (1997) Observations of Pa-231/U-235 disequilibrium in volcanic rocks. Earth Planet Sci Lett 148(1–2):259–271

Reid MR, Coath CD, Harrison TM, McKeegan KD (1997) Prolonged residence times for the youngest rhyolites associated with Long Valley Caldera: Th-230-U-238 ion microprobe dating of young zircons. Earth Planet Sci Lett 150(1–2):27–39

Reid MR, Vazquez JA, Schmitt AK (2011) Zircon-scale insights into the history of a Supervolcano, Bishop Tuff, Long Valley, California, with implications for the Ti-in-zircon geothermometer. Contrib Mineral Petrol 161(2):293–311

Roberts N, Reed JM, Leng JM, Kuzucuoglu C, Fontugne M, Bertaux J, Woldring H, Bottema S, Black S, Hunt E, Karabiyikoglu M (2001) The tempo of Holocene climatic change in the eastern Mediterranean region: new high-resolution crater-lake sediment data from central Turkey. Holocene 11(6):721–736

Rosman KJR, Taylor PDP (1998) Isotopic compositions of the elements. J Phys Chem Ref Data 27(6):1275–1287

Schmitt AK (2007) Ion microprobe analysis of (^{231}Pa)/(^{235}U) and an appraisal of protactinium partitioning in igneous zircon. Am Mineral 92(4):691–694

Schmitt AK, Grove M, Harrison TM, Lovera O, Hulen J, Walters M (2003) The Geysers—Cobb Mountain Magma System, California (Part 1): U-Pb zircon ages of volcanic rocks, conditions of zircon crystallization and magma residence times. Geochim Cosmochim Acta 67(18):3423–3442

Schmitt AK, Stockli DF, Niedermann S, Lovera OM, Hausback BP (2010) Eruption ages of Las Tres Vírgenes volcano (Baja California): a tale of two helium isotopes. Quatern Geochronol 5(5):503–511

Siebel W, Schmitt AK, Kiemele E, Danišík M, Aydin F (2011) Acigöl rhyolite field, central Anatolia (part II): geochemical and isotopic (Sr–Nd–Pb, δ^{18}O) constraints on volcanism involving two high-silica rhyolite suites. Contrib Mineral Petrol. doi: 10.1007/s00410-011-0651-2

Sieh K, Bursik M (1986) Most recent eruption of the mono craters, eastern central California. J Geophys Res Solid Earth Planets 91(B12):2539–2571

Simon JI, Reid MR (2005) The pace of rhyolite differentiation and storage in an 'archetypical' silicic magma system, Long Valley, California. Earth Planet Sci Lett 235(1–2):123–140

Simon JI, Renne PR, Mundil R (2008) Implications of pre-eruptive magmatic histories of zircons for U-Pb geochronology of silicic extrusions. Earth Planet Sci Lett 266(1–2):182–194

Simon JI, Vazquez JA, Renne PR, Schmitt AK, Bacon CR, Reid MR (2009) Accessory mineral U-Th-Pb ages and Ar-40/Ar-39 eruption chronology, and their bearing on rhyolitic magma evolution in the Pleistocene Coso volcanic field, California. Contrib Mineral Petrol 158(4):421–446

Slimak L, Kuhn SL, Roche H, Mouralis D, Buitenhuis H, Balkan-Atli N, Binder D, Kuzucuoglu C, Guillou H (2008) Kaletepe Deresi 3 (Turkey): Archaeological evidence for early human settlement in Central Anatolia. J Hum Evol 54(1):99–111

Temel A, Gundogdu MN, Gourgaud A (1998a) Petrological and geochemical characteristics of cenozoic high-K calc-alkaline volcanism in Konya, central Anatolia, Turkey. J Volcanol Geotherm Res 85(1–4):327–354

Temel A, Gundogdu MN, Gourgaud A, Le Pennec JL (1998b) Ignimbrites of Cappadocia (central Anatolia, Turkey): petrology and geochemistry. J Volcanol Geotherm Res 85(1–4):447–471

Toprak V (1998) Vent distribution and its relation to regional tectonics, Cappadocian Volcanics, Turkey. J Volcanol Geotherm Res 85(1–4):55–67

Toprak V, Göncüoğlu MC (1993) Tectonic control on the development of the Neogene-Quaternary central Anatolian volcanic province, Turkey. Geol J 28(3–4):357–369

Türkecan A, Kuzucuoğlu C, Mouralis D, Pastre J-F, Atıcı Y, Guillou H, Fontugne M (2004) Upper Pleistocene volcanism and palaeogeography in Cappadocia, Turkey. MTA-CNRS-TÜBİTAK 2001–2003 research programme. Tübitak project no. 101Y109, MTA report no. 10652, 180 pp

Vazquez JA, Reid MR (2002) Time scales of magma storage and differentiation of voluminous high-silica rhyolites at Yellowstone caldera, Wyoming. Contrib Mineral Petrol 144(3):274–285

Viereck-Goette L, Lepetit P, Gurel A, Ganskow G, Copuroglu I, Abratis M (2010) Revised volcanostratigraphy of the upper miocene to lower pliocene Urgup formation, Central Anatolian volcanic province, Turkey. Spec Pap Geol Soc Am 464:85–112

Wagner GA, Storzer D, Keller J (1976) Spaltspurendatierung quartärer Gesteinsgläser aus dem Mittelmeerraum. N Jb Miner Mh 2:84–94

Watson EB (1996) Dissolution, growth and survival of zircons during crustal fusion; kinetic principles, geological models and implications for isotopic inheritance. Spec Pap Geol Soc Am 315:43–56

Wiedenbeck M, Alle P, Corfu F, Griffin WL, Meier M, Oberli F, Vonquadt A, Roddick JC, Speigel W (1995) Three natural zircon standards for U-Th-Pb, Lu-Hf, Trace-Element and Ree Analyses. Geostand Newsl 19(1):1–23

Yıldırım T, Özgür R (1981) The Acigöl caldera. Jeomorfoloji Dergisi 10:59–70 (in Turkish with English abstract)